ResearchGate

See discussions, stats, and author profiles for this publication at: https://www.researchgate.net/publication/239942197

Exploiting Multivalent Nanoparticles for the Supramolecular Functionalization of Graphene with a Nonplanar Recognition Motif

ARTICLE *in* CHEMISTRY - A EUROPEAN JOURNAL · JULY 2013

Impact Factor: 5.73 · DOI: 10.1002/chem.201301102 · Source: PubMed

CITATIONS
5

READS
15

6 AUTHORS, INCLUDING:

Helena Isla
Institut des Sciences Chimiques de Rennes
10 PUBLICATIONS **229** CITATIONS
SEE PROFILE

Juan Aragó
The University of Warwick
32 PUBLICATIONS **158** CITATIONS
SEE PROFILE

Emilio M Pérez
Madrid Institute for Advanced Studies
75 PUBLICATIONS **2,171** CITATIONS
SEE PROFILE

Available from: Helena Isla
Retrieved on: 16 January 2016

CHEMISTRY
A EUROPEAN JOURNAL

FULL PAPER

DOI: 10.1002/chem.201301102

Exploiting Multivalent Nanoparticles for the Supramolecular Functionalization of Graphene with a Nonplanar Recognition Motif

Fulvio G. Brunetti,[a] Helena Isla,[b] Juan Aragó,[c] Enrique Ortí,*[c] Emilio M. Pérez,*[a] and Nazario Martín*[a, b]

Abstract: The supramolecular modification of planar graphene with the geometrically mismatched, curved 9,10-di(1,3-dithiole-2-ylidene)-9,10-dihydroanthracene (exTTF) molecule is demonstrated. The exTTF–graphene interaction is governed by π–π and CH–π interactions, with a negligible contribution from charge transfer. We amplified these weak forces through multivalent gold nanoparticles. Our results show that planarity is not a prerequisite for recognition motifs for graphene.

Keywords: graphene · multivalency · nanoparticles · pi–pi interactions · supramolecular chemistry.

Introduction

Monolayer graphene is a 2D lattice of carbon atoms arranged in a honeycomb structure.[1] More generally, few-layer graphene (FLG) can be defined as less than 10 layers of graphene. The extraordinary structural and physical properties of graphene have rightly made it the object of a very intense multidisciplinary research effort, in which physics has so far played the leading role.[2] In particular, graphene's electronic properties have been the focus of a significant number of investigations.[3] In comparison, the chemistry of graphene is not as well-developed.[4] From a synthetic point of view, important breakthroughs include the synthesis of graphene through sublimation of Si from SiC,[5] the chemical vapor deposition (CVD) of gaseous carbon sources on metal catalysts,[6] the reduction of graphene oxide (RGO),[7] the "unzipping" of carbon nanotubes to produce graphene nanoribbons,[8] and the synthesis of monodisperse nanographenes (or large polycyclic aromatic hydrocarbons, PAHs).[9] Recently, the synthesis of graphene from inexpensive carbon sources through CVD has been described.[10]

[a] Dr. F. G. Brunetti, Dr. E. M. Pérez, Prof. Dr. N. Martín
IMDEA-Nanoscience
C/Faraday, 9. Ciudad Universitaria de Cantoblanco
28049 Madrid (Spain)
E-mail: emilio.perez@imdea.org

[b] H. Isla, Prof. Dr. N. Martín
Departmento de Química Orgánica, Facultad de Ciencias Químicas
Universidad Complutense de Madrid
Avenida Complutense s/n, 28040 Madrid (Spain)
Fax: (+34) 91-394-4103
E-mail: nazmar@quim.ucm.es
Homepage: http://www.ucm.es/info/fullerene/

[c] Dr. J. Aragó, Prof. Dr. E. Ortí
Instituto de Ciencia Molecular
Universidad de Valencia, Paterna, 46980 Valencia (Spain)
E-mail: enrique.orti@uv.es

Supporting information for this article is available on the WWW under http://dx.doi.org/10.1002/chem.201301102.

The toolbox of reactions for the chemical manipulation of graphene is more limited.[4a,d,e] The covalent modification of graphene's basal planes through its reaction with aryl diazonium salts[11] and 1,3-dipoles[4e,12] has been reported. With regard to its noncovalent or supramolecular modification, the interaction of graphene with surfactants[13] and planar aromatic moieties, including PAHs,[14] pyrene,[15] tetracyano-*p*-quinodimethane,[16] and phthalocyanines,[17] has been described.

We have previously exploited the concave geometry of 9,10-di(1,3-dithiole-2-ylidene)-9,10-dihydroanthracene (exTTF) to synthesize hosts for fullerenes[18] and a variety of fullerene–exTTF self-assembled nanostructures that profit from the concave–convex complementarity of the systems.[19] In the field of molecular recognition of fullerenes, there are numerous examples of hosts that exploit planar aromatic moieties (particularly porphyrins) to recognize the convex surface of the fullerene guests, despite the planar–convex surface mismatch.[20] The same is true for the supramolecular chemistry of carbon nanotubes, where pyrene is by far the most widely used recognition motif.[21] Inspired by this fact, we contemplated the possibility that exTTF could establish positive noncovalent interactions with planar graphene, regardless of its biconcave geometry.[22] So far, it has not been established whether planarity is an essential condition for the structure of recognition motifs for graphene. In this article, we prove that this is not the case, by demonstrating the noncovalent modification of graphene with a nonplanar recognition motif, exTTF.

Results and Discussion

To explore the interaction between exTTF and planar graphene, we first carried out density functional theory (DFT) calculations on an exTTF–graphene model, in which the exTTF unit was placed in different orientations with respect to a PAH graphene-like molecule including 31 benzene

 © 2013 Wiley-VCH Verlag GmbH & Co. KGaA, Weinheim

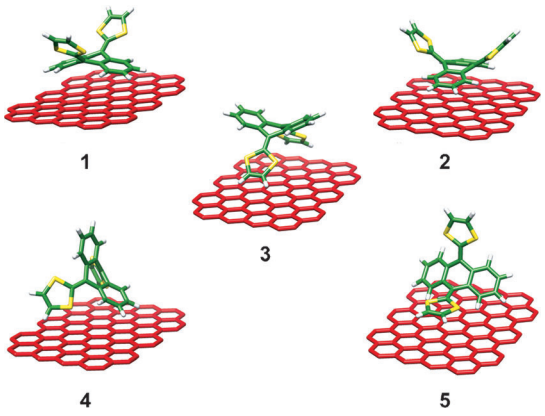

Figure 1. Minimum-energy structures computed for the exTTF–graphene models (**1**–**5**) at the revPBE0-D3/cc-pVDZ level. Carbon atoms of exTTF are depicted in green, sulfur in yellow, and hydrogen in white. Carbon atoms of the graphene sheet are depicted in red, and hydrogen atoms have been omitted for clarity.

rings ($C_{84}H_{24}$). Calculations were performed using the revPBE0-D3 functional,[23] which is able to capture dispersion effects and is one of the best functionals to accurately describe supramolecular complexes governed by π–π interactions (see the Supporting Information for computational details).[24] Figure 1 displays the minimum-energy structures (**1**–**5**) calculated for the exTTF–graphene supramolecular interaction at the revPBE0-D3/cc-pVDZ level. More detailed pictures of the orientation of exTTF with respect to the graphene sheet are given in Figures S1–S5 in the Supporting Information. In structures **1** and **2** the interaction of the exTTF fragment with graphene mainly occurs through the concave anthracene backbone, whereas in structure **3** the interaction takes place through the concave dithiole face. Structures **1** and **2** are mainly determined by π–π interactions, whereas structure **3** involves close CH–π interactions (ca. 2.7 Å) between the terminal hydrogen atoms of the dithiole rings and the graphene sheet. The exTTF molecule can also interact with the graphene sheet through a benzene ring and the sulfur atoms (structure **4**), or through a dithiole ring (structure **5**). Structures **4** and **5** imply a mixture of π–π and CH–π interactions. All optimized structures **1**–**5** show close intermolecular distances in the 3.1–4.0 Å range (see Figures S1–S5 in the Supporting Information), which are the structural signature of positive noncovalent interactions. Remarkably, despite the electron-donor character of exTTF, our calculations predict negligible contributions from charge-transfer interactions (< 0.005 e).

To estimate the binding energies of the exTTF–graphene models **1**–**5**, single-point energy calculations were performed on the previously optimized structures using the revPBE0-D3 functional and the more extended triple-ζ cc-pVTZ basis set (see computational details). Structures **4** and **5** are found to be the most stable, with binding energies of −22.2 and −25.2 kcal mol^{-1}, respectively. Structures **1**, **2**, and **3** also exhibit significant binding energies of −19.0, −20.7, and −16.8 kcal mol^{-1}, respectively. To discard possible undesirable terminal effects from the limited size of the PAH used to model the graphene sheet, an exTTF–graphene model based on structure **1** with a larger PAH ($C_{104}H_{28}$) was also calculated (Figure S6 in the Supporting Information). The binding energy for the larger exTTF–graphene model is −19.3 kcal mol^{-1}, which is similar to that obtained for structure **1** (−19.0 kcal mol^{-1}). These results confirm that the size of the PAH ($C_{84}H_{24}$) used to model the graphene sheet is appropriate to compute the association energies between exTTF and graphene. To investigate the influence of the nonplanar geometry of exTTF on the supramolecular association with graphene, the interaction of the graphene sheet with a planar π-conjugated motif, such as anthracene (the central backbone of exTTF), was also computed in an eclipsed-like disposition similar to structure **1** (Figure S7 in the Supporting Information). The binding energy computed at the revPBE0-D3/cc-pVTZ level for this anthracene–graphene model is −20.4 kcal mol^{-1}, which is higher than that computed for its homologous structure **1** but is significant smaller than those computed for structures **4** and **5**. The remarkable increase of the binding energies for structures **4** and **5** with respect to the anthracene–graphene model clearly reveals that the planarity of the π-conjugated motif does not necessarily favor a stronger supramolecular association with a graphene sheet. For instance, despite the concave–planar surface mismatch, the exTTF system can orient in different ways to interact strongly with a graphene sheet.

Experimentally (UV/Vis titration, Figure S8 in the Supporting Information), we found that a single unit of exTTF does not produce detectable interactions with graphene,[18a] so we decided to employ a multivalent approach to amplify them, in which gold nanoparticles would serve as a scaffold to present multiple units of exTTF to the surface of graphene. Multivalent interactions are often much stronger than the corresponding sum of the monovalent ones, a strategy that nature exploits in multiple recognition events, for example, in the recognition of polysaccharides by lectins.[25] Another advantage of this strategy is that gold nanoparticles can be utilized to track the interaction with graphene through UV/Vis spectroscopy and transmission electron microscopy (TEM).[12] We have recently reported the synthesis of gold nanoparticles capped with multiple units of exTTF.[26] In the batch utilized for these experiments, the exTTF gold nanoparticles (exTTFAuNPs, Figure 2) showed an average diameter of (7.1 ± 0.9) nm in TEM analysis, with 567 ± 41 exTTF units per nanoparticle. As a control, we also synthesized nanoparticles capped with the ethyl ester of mercaptoundecanoic acid (ethylAuNPs, Figure 2). The nanoparticles were characterized by UV/Vis, FTIR, TEM, atomic force microscopy (AFM), and thermogravimetric analysis (TGA). For full experimental details and characterization, see the Supporting Information.

Complete removal of the oxygen-containing moieties in RGO is problematic.[7] To avoid interactions that might arise from residual oxygenated moieties, we decided to obtain FLG from the exfoliation of graphite, following a procedure previously described by Coleman et al.[27] Typical TEM micrographs and the Raman spectrum of the obtained

 © 2013 Wiley-VCH Verlag GmbH & Co. KGaA, Weinheim

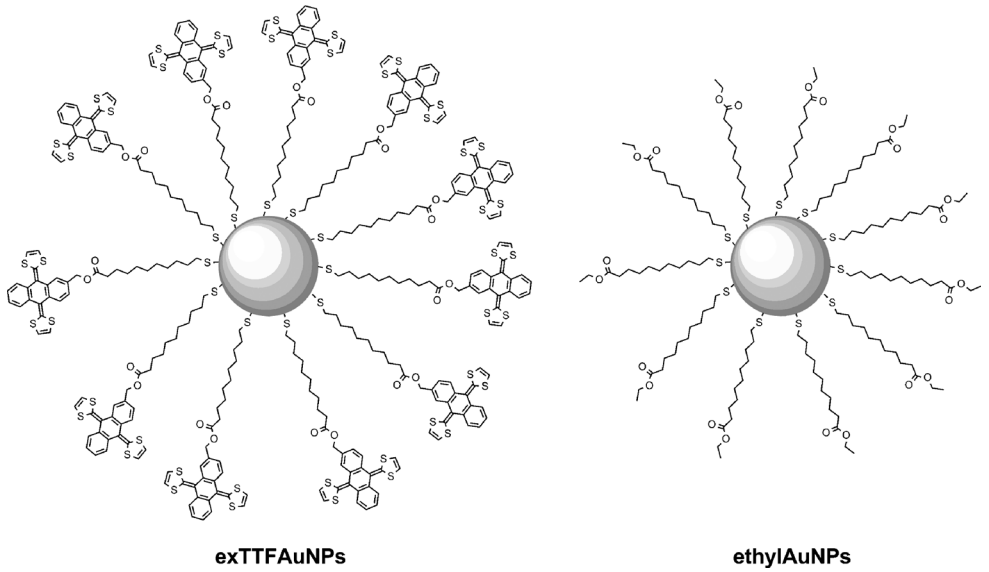

Figure 2. Structures of exTTFAuNPs and ethylAuNPs.

FLG are shown in Figure S9 in the Supporting Information. The images and spectroscopy data are consistent with ≤ 4 layers of graphene. In particular, the G′ band requires five Lorentzians of about 24 cm^{-1} full width at half maximum (FWHM) to be fitted, indicative of 3 layer graphene.[28]

In order to investigate the interaction between exTTFAuNPs and FLG in solution, we carried out a UV/Vis titration. To a suspension of exTTFAuNPs in chlorobenzene (1 mL), we added aliquots of a suspension of FLG in chlorobenzene (5 μL). The resulting mixtures were sonicated for 15 min to allow for complete mixing prior to registration of their spectra.[29] The results are shown in Figure 3a. Upon addition of FLG to the solution of exTTFAuNPs, significant changes are observed in their UV/Vis spectrum that point to a substantial exTTFAuNP–graphene interaction. In particular, we observed a decrease in the intensity of the band at $\lambda = 437$ nm, assigned to the exTTF chromophore, depletion of the plasmon band at $\lambda = 564$ nm, and an increase of the featureless absorption in the 700–1000 nm region, due to absorption and/or dispersion from FLG. These changes occur with the formation of a pseudo-isosbestic point at approximately 650 nm. We have previously found similar spectroscopic changes in the association of fullerene with exTTFAuNPs.[26] In particular, the decrease in the absorbance of exTTF at 437 nm is the spectroscopic signature of the binding of exTTF hosts with fullerene guests.[18] The decrease in intensity of the plasmon resonance band can be ascribed to a change in the aggregation state of the nanoparticles and/or to a change in the dielectric function of the surrounding media upon association.[26,30]

When the same titration experiment was carried out with ethylAuNPs, the spectra obtained were approximately the arithmetic addition of the spectra of ethylAuNPs and FLG (Figure 3b). This result indicates the absence of interactions between ethylAuNPs and graphene, which confirms the specificity of the exTTF–graphene assembly.

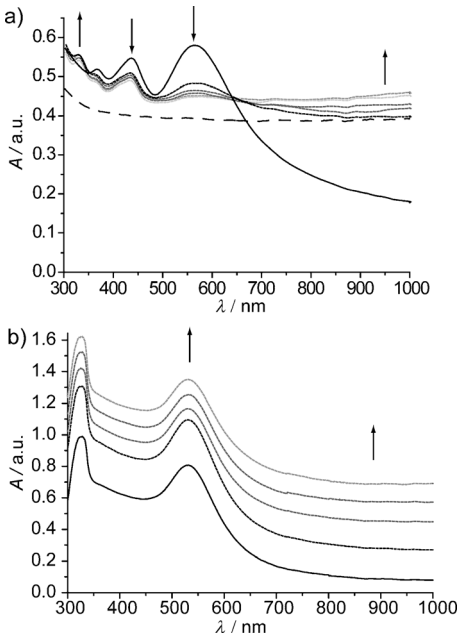

Figure 3. a) Black solid and grey dotted lines: UV/Vis spectra obtained during the titration of exTTFAuNPs (ca. 0.33 mg mL^{-1}, 1 mL, chlorobenzene, RT) with aliquots of a suspension of FLG (5 μL each, 0–25 μL total volume, ca. 1 mg mL^{-1}, chlorobenzene, RT). Dashed line: UV/Vis spectrum of an aliquot of FLG (25 μL) dissolved in chlorobenzene (1 mL). b) UV/Vis spectra obtained during the titration of ethylAuNPs (0.5 mg mL^{-1}, 1 mL chlorobenzene, RT) with aliquots of a suspension of FLG (5 μL each, 0–25 μL total volume, ca. 1 mg mL^{-1}, chlorobenzene, RT).

To visualize the association, an aliquot of the final solution in the UV/Vis titration experiment was drop-cast onto a carbon-coated copper TEM grid. Examples of the typical micrographs obtained are shown in Figure 4a–d and Figure S10 in the Supporting Information. The basal planes of graphene are heavily functionalized with exTTFAuNPs, which are concentrated in regions with a higher number of

 © 2013 Wiley-VCH Verlag GmbH & Co. KGaA, Weinheim

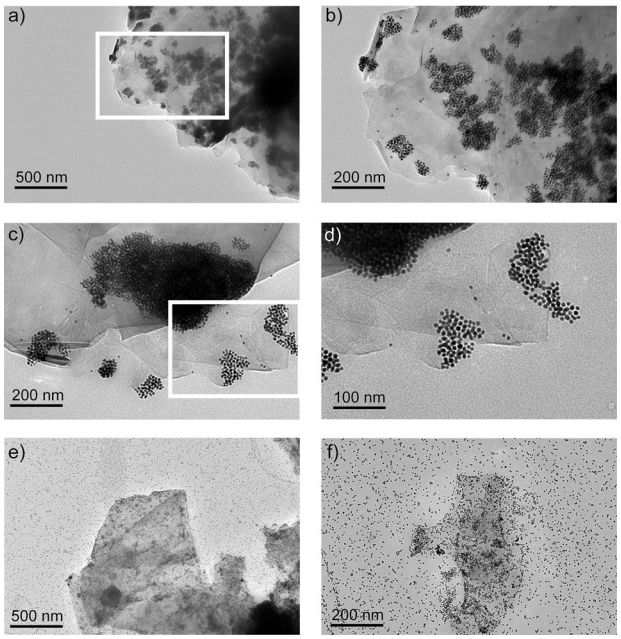

Figure 4. a)–d) TEM micrographs of exTTFAuNPs–FLG associates: b) and d) are higher magnification images of the regions marked with white rectangles in a) and c), respectively; e) and f) are TEM micrographs of a mixture of ethylAuNPs and FLG.

graphene layers (Figure 4a and b). A close examination of the micrographs suggests that the nanoparticles are localized between layers of graphene (Figure 4c and d), a situation in which the exTTFAuNPs–graphene noncovalent interactions are maximized. We observed neither free exTTFAuNPs nor unfunctionalized FLG flakes, suggesting a very strong binding event. In contrast, and in agreement with the UV/Vis experiments, TEM scrutiny of an analogous mixture of ethylAuNPs and FLG revealed a random distribution of nanoparticles across the graphene flakes and the surrounding area (Figure 4e and f, Figure S11 in the Supporting Information).

Raman and energy-dispersive X-ray diffraction (EDX) spectroscopy also support the functionalization. In the Raman spectrum of the exTTFAuNPs–FLG associate, signals at 2800–3000 and about 1470 cm^{-1} were observed, corresponding to the alkyl moieties in the exTTFAuNPs, in addition to the D, G, and G′ bands of the graphitic material (Figure 5a). We also observed a shift towards higher wavenumbers in the G band of 4 cm^{-1}, compared with pristine FLG (Figure 5b). These changes are consistent with the supramolecular modification of FLG through weak dispersion-type interactions,[31] without significant charge-transfer,[14] as predicted by theory. Remarkably, the G′ band still requires six Lorentzians of FWHM = 24 cm^{-1} to be fitted correctly, proving that there is little or no graphitization of the sample during the titration experiments.

EDX shows the presence of a significant amount of gold (Figure 5c), which was confirmed to be confined to the exTTFAuNPs through STEM with EDX elemental distribution (Figure 6). All these data are fully consistent with the supramolecular functionalization.

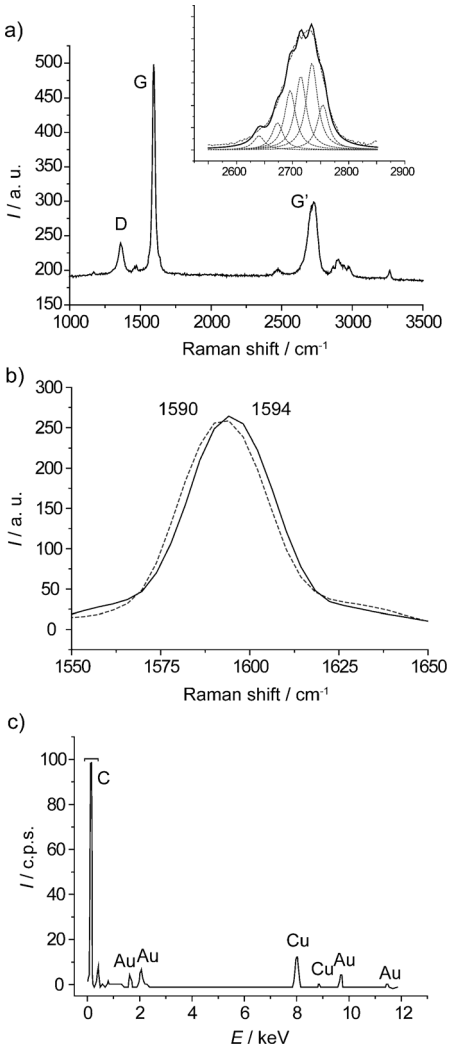

Figure 5. a) Raman spectra ($\lambda_{exc.}$ = 532 nm, 0.8 mW, 100x optical lens) of the exTTFAuNPs–FLG associate. Inset shows the fit of the G′ band to six Lorentzians of FWHM = 24 cm^{-1}. b) Zoom in on the G band of FLG (black) and exTTFAuNPs–FLG (dashed grey line). c) EDX spectrum of the exTTFAuNPs–FLG associate.

To determine if the exTTFAuNPs are located in between or on top of the graphene layers, we carried out scanning electron (SEM) and atomic force microscopy (AFM). SEM of the as obtained FLG revealed flakes composed of several layers of graphene, as expected (Figure S12 in the Supporting Information). Figure 7a and b shows SEM imaging of a flake of exTTFAuNPs–FLG at different beam potentials (5 and 10 kV). The surface of FLG is mostly clean, with a few nanoparticle clusters scattered on it. On the contrary, where graphene has folded over, several clusters of exTTFAuNPs can be seen (marked with a white circle in Figure 7a and b). Upon doubling the intensity of the beam potential, these clusters become more visible, indicating that they are placed between the graphene layers.

Likewise, AFM revealed FLG flakes with heights of 12–50 nm and fundamentally clean, flat surfaces (Figure 7c and d). Luckily, one of the flakes presented a hole in which sev-

 © 2013 Wiley-VCH Verlag GmbH & Co. KGaA, Weinheim

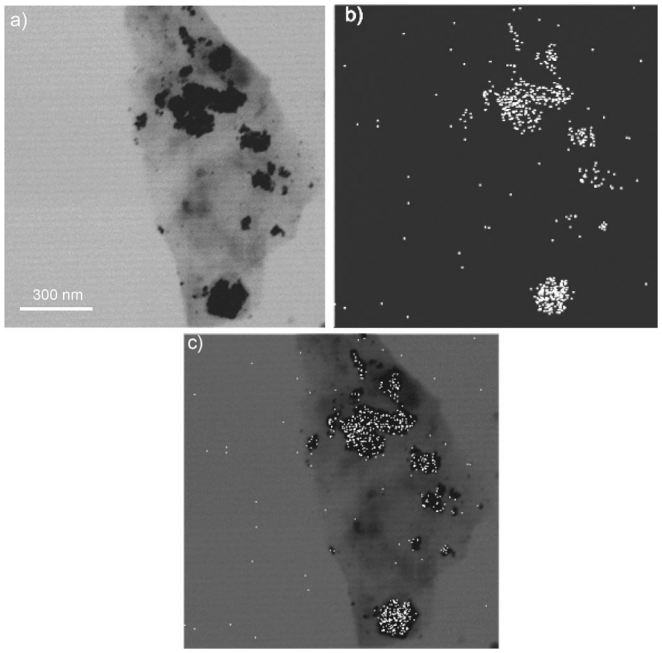

Figure 6. a) STEM micrograph of the exTTFAuNPs–FLG associate; b) elemental distribution (EDX) of gold in the same image; and c) combined images.

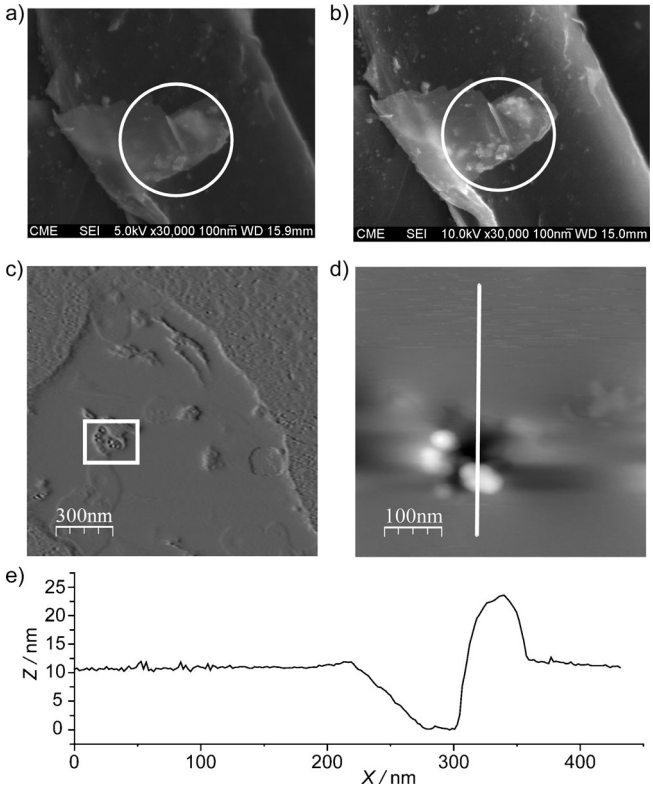

Figure 7. a) SEM micrograph of exTTFAuNPs–FLG at a beam potential of 5.0 kV. b) SEM micrograph of exTTF–AuNPs–FLG at a beam potential of 10.0 kV. White circles mark the area where a cluster of exTTFAuNPs is visible underneath a graphene layer. c) AFM phase image of a FLG flake. d) Higher magnification AFM topographic image of the area in the white rectangle in c). e) Profile along the white line in d).

eral exTTFAuNPs could be seen. A closer inspection of this area is shown in Figure 7d. The topographic profile along the white line depicted in Figure 7d reveals a step of −11 nm, consistent with two layers of FLG separated by one layer of exTTFAuNPs, followed by an increase in height of approximately 23 nm, revealing the presence of a conglomerate of nanoparticles. These findings are concordant with the formation of graphene–exTTFAuNPs–graphene sandwich-type nanostructures. The prevalence of this type of structure can be explained by its thermodynamic stability compared with the situation in which the exTTFAuNPs lay on top of graphene. In the sandwich-type structure, the exTTF–graphene interactions are maximized, whereas if the exTTFAuNPs lay on top of grapheme, it would leave many possible exTTF–graphene interaction points unsatisfied.

Conclusion

In conclusion, we have found that the biconcave exTTF molecule serves as an efficient recognition motif for graphene, allowing for its noncovalent modification despite the geometric disparity. The positive exTTF–graphene interaction is supported by DFT calculations, which indicate that it is based on π–π and CH–π interactions, with no contribution from charge transfer. These findings were corroborated by Raman spectroscopy. The magnitude of the exTTF–graphene interaction is even greater than that of a similar but planar molecule, anthracene, proving that planarity is not a prerequisite for the structure of supramolecular partners for graphene. Similar convex–planar mismatched supramolecular pairs are frequent in the noncovalent chemistry of fullerenes and carbon nanotubes,[20,21] but had not been observed previously for graphene.

The use of gold nanoparticles as scaffolds to present multiple units of exTTF to the surface of graphene allowed us to magnify the exTTF–graphene interaction through a multivalent effect. The properties of the gold nanoparticles were also exploited to track the recognition event. Scrutiny under TEM, Raman, STEM, SEM, and AFM of the exTTFAuNPs–graphene associates strongly suggests that these are graphene–exTTFAuNPs–graphene sandwich-type nanostructures.

Our findings expand the number of possible recognition motifs for graphene to a great extent. The changes to the electronic properties of graphene brought about by its noncovalent modification with the electron donor exTTF and the possible applications of the resulting material will be the subject of our future investigations.

Acknowledgements

We are thankful to A. Soubrié, A. Rodríguez, J. L. Baldonedo, and A. del Campo for assistance with AFM, SEM, STEM, and Raman, respectively.

 © 2013 Wiley-VCH Verlag GmbH & Co. KGaA, Weinheim

This work has been supported by the MICINN of Spain (CTQ2011-25714, CTQ2011-24652, CTQ2012-31914, PIB2010JP-00196, and Consolider-Ingenio CSD2007-00010 on Molecular Nanoscience), the CAM (MADRISOLAR-2 S2009/PPQ-1533), and the Generalitat Valenciana (PROMETEO/2012/053). F.G.B., H.I., and E.M.P. thank the MINECO for a Juan de la Cierva postdoctoral fellowship, a FPU studentship and a Ramón y Cajal fellowship cofinanced by the European Social Fund, respectively.

[1] a) A. K. Geim, K. S. Novoselov, *Nat. Mater.* **2007**, *6*, 183–191; b) M. J. Allen, V. C. Tung, R. B. Kaner, *Chem. Rev.* **2010**, *110*, 132–145.

[2] a) A. K. Geim, *Angew. Chem.* **2011**, *123*, 7100–7122; *Angew. Chem. Int. Ed.* **2011**, *50*, 6966–6985; b) K. S. Novoselov, *Angew. Chem.* **2011**, *123*, 7123–7141; *Angew. Chem. Int. Ed.* **2011**, *50*, 6986–7002.

[3] a) C. N. R. Rao, A. K. Sood, K. S. Subrahmanyam, A. Govindaraj, *Angew. Chem.* **2009**, *121*, 7890–7916; *Angew. Chem. Int. Ed.* **2009**, *48*, 7752–7777; b) Ph. Avouris, *Nano Lett.* **2010**, *10*, 4285–4294; c) S. Pang, Y. Hernandez, X. Feng, K. Müllen, *Adv. Mater.* **2011**, *23*, 2779–2795; d) E. Bekyarova, S. Sarkar, F. Wang, M. E. Itkis, I. Kalinina, X. Tian, R. C. Haddon, *Acc. Chem. Res.* **2013**, *46*, 65–76.

[4] a) Z. Sun, D. K. James, J. M. Tour, *J. Phys. Chem. Lett.* **2011**, *2*, 2425–2432; b) Y. Chen, B. Zhang, G. Liu, X. Zhuang, E.-T. Kang, *Chem. Soc. Rev.* **2012**, *41*, 4688–4707; c) C. K. Chua, M. Pumera, *Chem. Soc. Rev.* **2013**, *42*, 3222–3233; d) J. Park, M. Yan, *Acc. Chem. Res.* **2013**, *46*, 181–189; e) M. Quintana, E. Vázquez, M. Prato, *Acc. Chem. Res.* **2013**, *46*, 138–148; f) L. Rodríguez-Pérez, M. A. Herranz, N. Martín, *Chem. Commun.* **2013**, *49*, 3721–3735.

[5] K. V. Emtsev, A. Bostwick, K. Horn, J. Jobst, G. L. Kellogg, L. Ley, J. L. McChesney, T. Ohta, S. A. Reshanov, J. Roehrl, E. Rotenberg, A. K. Schmid, D. Waldmann, H. B. Weber, T. Seyller, *Nat. Mater.* **2009**, *8*, 203–207.

[6] a) A. L. Vázquez de Parga, F. Calleja, B. Borca, M. C. G. Passeggi Jr, J. J. Hinarejos, F. Guinea, R. Miranda, *Phys. Rev. Lett.* **2008**, *100*, 056807; b) K. S. Kim, Y. Zhao, H. Jang, S. Y. Lee, J. M. Kim, K. S. Kim, J.-H. Ahn, P. Kim, J.-Y. Choi, B. H. Hong, *Nature* **2009**, *457*, 706–710; c) X. Li, W. Cai, J. An, S. Kim, J. Nah, D. Yang, R. Piner, A. Velamakanni, I. Jung, E. Tutuc, S. K. Banerjee, L. Colombo, R. S. Ruoff, *Science* **2009**, *324*, 1312–1314.

[7] D. R. Dreyer, S. Park, C. W. Bielawski, R. S. Ruoff, *Chem. Soc. Rev.* **2010**, *39*, 228–240.

[8] D. V. Kosynkin, A. L. Higginbotham, A. Sinitskii, J. R. Lomeda, A. Dimiev, B. K. Price, J. M. Tour, *Nature* **2009**, *458*, 872–876.

[9] a) P. Samori, N. Severin, C. D. Simpson, K. Müllen, J. P. Rabe, *J. Am. Chem. Soc.* **2002**, *124*, 9454–9457; b) M. Kastler, J. Schmidt, W. Pisula, D. Sebastiani, K. Müllen, *J. Am. Chem. Soc.* **2006**, *128*, 9526–9534; c) K. Müllen, J. P. Rabe, *Acc. Chem. Res.* **2008**, *41*, 511–520.

[10] G. Ruan, Z. Sun, Z. Peng, J. M. Tour, *ACS Nano* **2011**, *5*, 7601–7607.

[11] a) J. R. Lomeda, C. D. Doyle, D. V. Kosynkin, W.-F. Hwang, J. M. Tour, *J. Am. Chem. Soc.* **2008**, *130*, 16201–16206; b) E. Bekyarova, M. E. Itkis, P. Ramesh, C. Berger, M. Sprinkle, W. A. de Heer, R. C. Haddon, *J. Am. Chem. Soc.* **2009**, *131*, 1336–1337; c) G. L. C. Paulus, Q. H. Wang, M. S. Strano, *Acc. Chem. Res.* **2013**, *46*, 160–170.

[12] a) M. Quintana, K. Spyrou, M. Grzelczak, W. R. Browne, P. Rudolf, M. Prato, *ACS Nano* **2010**, *4*, 3527–3533; b) M. Quintana, A. Montellano, A. E. del Río Castillo, G. Van Tendeloo, C. Bittencourt, M. Prato, *Chem. Commun.* **2011**, *47*, 9330–9332.

[13] M. Lotya, Y. Hernandez, P. J. King, R. J. Smith, V. Nicolosi, L. S. Karlsson, F. M. Blighe, S. De, Z. Wang, I. T. McGovern, G. S. Duesberg, J. N. Coleman, *J. Am. Chem. Soc.* **2009**, *131*, 3611–3620.

[14] Q. Su, S. Pang, V. Alijani, C. Li, X. Feng, K. Müllen, *Adv. Mater.* **2009**, *21*, 3191–3195.

[15] J. A. Mann, J. Rodríguez-López, H. D. Abruña, W. R. Dichtel, *J. Am. Chem. Soc.* **2011**, *133*, 17614–17617.

[16] a) S. Barja, M. Garnica, J. J. Hinarejos, A. L. Vázquez de Parga, N. Martín, R. Miranda, *Chem. Commun.* **2010**, *46*, 8198–8200; b) M. Garnica, D. Stradi, S. Barja, F. Calleja, C. Díaz, M. Alcamí, N. Martín, A. L. Vázquez de Parga, F. Martín, R. Miranda, *Nat. Phys.* **2013**, *9*, 368–374.

[17] J. Malig, N. Jux, D. Kiessling, J.-J. Cid, P. Vazquez, T. Torres, D. M. Guldi, *Angew. Chem.* **2011**, *123*, 3623–3627; *Angew. Chem. Int. Ed.* **2011**, *50*, 3561–3565.

[18] a) E. M. Pérez, L. Sánchez, G. Fernández, N. Martín, *J. Am. Chem. Soc.* **2006**, *128*, 7172–7173; b) E. M. Pérez, A. L. Capodilupo, G. Fernández, L. Sánchez, P. M. Viruela, R. Viruela, E. Ortí, M. Bietti, N. Martín, *Chem. Commun.* **2008**, 4567–4569; c) S. S. Gayathri, M. Wielopolski, E. M. Pérez, G. Fernández, L. Sánchez, R. Viruela, E. Ortí, D. M. Guldi, N. Martín, *Angew. Chem.* **2009**, *121*, 829–834; *Angew. Chem. Int. Ed.* **2009**, *48*, 815–819; d) E. Huerta, H. Isla, E. M. Pérez, C. Bo, N. Martín, J. de Mendoza, *J. Am. Chem. Soc.* **2010**, *132*, 5351–5353; e) H. Isla, M. Gallego, E. M. Pérez, R. Viruela, E. Ortí, N. Martín, *J. Am. Chem. Soc.* **2010**, *132*, 1772–1773; f) D. Canevet, M. Gallego, H. Isla, A. de Juan, E. M. Pérez, N. Martín, *J. Am. Chem. Soc.* **2011**, *133*, 3184–3190; g) B. Grimm, H. Isla, E. M. Pérez, N. Martín, D. M. Guldi, *Chem. Commun.* **2011**, *47*, 7449–7451.

[19] a) G. Fernández, E. M. Pérez, L. Sánchez, N. Martín, *Angew. Chem.* **2008**, *120*, 1110–1113; *Angew. Chem. Int. Ed.* **2008**, *47*, 1094–1097; b) G. Fernández, E. M. Pérez, L. Sánchez, N. Martín, *J. Am. Chem. Soc.* **2008**, *130*, 2410–2411; c) G. Fernández, L. Sanchez, E. M. Pérez, N. Martin, *J. Am. Chem. Soc.* **2008**, *130*, 10674–10683; d) J. Santos, E. M. Pérez, B. M. Illescas, N. Martin, *Chem. Asian J.* **2011**, *6*, 1848–1853.

[20] a) K. Tashiro, T. Aida, *Chem. Soc. Rev.* **2007**, *36*, 189–197; b) E. M. Pérez, N. Martin, *Chem. Soc. Rev.* **2008**, *37*, 1512–1519; c) D. Canevet, E. M. Pérez, N. Martín, *Angew. Chem.* **2011**, *123*, 9416–9427; *Angew. Chem. Int. Ed.* **2011**, *50*, 9248–9259.

[21] a) N. Nakashima, Y. Tomonari, H. Murakami, *Chem. Lett.* **2002**, 638–639; b) M. Á. Herranz, C. Ehli, S. Campidelli, M. Gutiérrez, G. L. Hug, K. Ohkubo, S. Fukuzumi, M. Prato, N. Martín, D. M. Guldi, *J. Am. Chem. Soc.* **2008**, *130*, 66–73.

[22] S. P. Economopoulos, G. Rotas, Y. Miyata, H. Shinohara, N. Tagmatarchis, *ACS Nano* **2010**, *4*, 7499–7507.

[23] a) Y. Zhang, W. Yang, *Phys. Rev. Lett.* **1998**, *80*, 890–890; b) S. Grimme, J. Antony, S. Ehrlich, H. Krieg, *J. Chem. Phys.* **2010**, *132*, 154104–154119.

[24] W. Hujo, S. Grimme, *J. Chem. Theory Comput.* **2011**, *7*, 3866–3871.

[25] a) J. D. Badjic, A. Nelson, S. J. Cantrill, W. B. Turnbull, J. F. Stoddart, *Acc. Chem. Res.* **2005**, *38*, 723–732; b) C. Fasting, C. A. Schalley, M. Weber, O. Seitz, S. Hecht, B. Koksch, J. Dernedde, C. Graf, E.-W. Knapp, R. Haag, *Angew. Chem.* **2012**, *124*, 10622–10650; *Angew. Chem. Int. Ed.* **2012**, *51*, 10472–10498; c) J. Luczkowiak, A. Muñoz, M. Sánchez-Navarro, R. Ribeiro-Viana, A. Ginieis, B. M. Illescas, N. Martín, R. Delgado, J. Rojo, *Biomacromolecules* **2013**, *14*, 431–437.

[26] R. Cao, Jr., H. Isla, R. Cao, E. M. Perez, N. Martin, *Chem. Sci.* **2011**, *2*, 1384–1388.

[27] a) Y. Hernández, V. Nicolosi, M. Lotya, F. M. Blighe, Z. Sun, S. De, I. T. McGovern, B. Holland, M. Byrne, Y. K. Gun′Ko, J. J. Boland, P. Niraj, G. Duesberg, S. Krishnamurthy, R. Goodhue, J. Hutchison, V. Scardaci, A. C. Ferrari, J. N. Coleman, *Nat. Nanotechnol.* **2008**, *3*, 563–568; b) J. N. Coleman, *Acc. Chem. Res.* **2013**, *46*, 14–22.

[28] L. M. Malard, M. A. Pimenta, G. Dresselhaus, M. S. Dresselhaus, *Phys. Rep.* **2009**, *473*, 51–87.

[29] K. R. Moonoosawmy, P. Kruse, *J. Am. Chem. Soc.* **2008**, *130*, 13417–13424.

[30] M. A. García, *J. Phys. D* **2011**, *44*, 283001.

[31] S. K. Samanta, K. S. Subrahmanyam, S. Bhattacharya, C. N. R. Rao, *Chem. Eur. J.* **2012**, *18*, 2890–2901.

Received: March 21, 2013
Published online: June 17, 2013

 © 2013 Wiley-VCH Verlag GmbH & Co. KGaA, Weinheim